ChemComm

Cite this: *Chem. Commun.*, 2012, **48**, 3354–3356

www.rsc.org/chemcomm

COMMUNICATION

Ultrasensitive and selective detection of nicotinamide adenine dinucleotide by target-triggered ligation–rolling circle amplification†

Yongxi Zhao,*[a] Lin Qi,[a] Feng Chen,[a] Yanhua Dong,[a] Yu Kong,[a] Yayan Wu[a] and Chunhai Fan*[b]

Received 28th November 2011, Accepted 7th February 2012
DOI: 10.1039/c2cc17422g

An ultrasensitive fluorescence assay for nicotinamide adenine dinucleotide (NAD^+) was developed by target-triggered ligation–rolling circle amplification (L-RCA). This novel approach can detect as low as 1 pM NAD^+, much lower than those of previously reported biosensors, and exhibits high discrimination ability even against 200 times excess of NAD^+ analogs.

Nicotinamide adenine dinucleotide (NAD^+), a ubiquitous biological molecule, participates in many biological processes and plays a crucial role in cell proliferation, apoptosis, transcriptional regulation, DNA repair, calcium homeostasis, and calorie-restriction mediated life-span extension.[1] It functions as a cofactor of numerous redox reactions as well as a consumable substrate for several classes of NAD^+-dependent enzymes.[2] Abnormal changes in NAD^+ levels and/or the NAD^+/reduced nicotinamide adenine dinucleotide (NADH) ratios correlate with several age-associated diseases, such as cancer, diabetes, and neurodegenerative diseases.[1d,3] Therefore, the development of a NAD^+ assay is of great significance for clinical diagnosis and therapy as well as understanding its roles in biological processes.

Traditional approach for NAD^+ determination is based on an enzymatic cycling strategy, allowing a sensitivity of picomolar range per assay.[4] Since both NAD^+ and NADH can initiate the cycling, the assay is unable to discriminate NAD^+ from NADH or other analogues. The accurate determination of NAD^+ in a single cell has been reported by combining the sensitivity of enzymatic cycling assay with the separation power of capillary electrophoresis.[5] Other alternative strategies have also been developed for NAD^+ detection, such as high performance liquid chromatography coupled with electrospray ionization tandem mass spectrometry (HPLC-ESI-MS/MS),[6] HPLC-UV detection,[7] carbon 13 nuclear magnetic resonance (^{13}CNMR) spectrometry,[8] and fluorescence methods.[9] Unfortunately, these methods are either extremely complicated, not selective enough for practical applications, or lacking sensitivity and requiring expensive equipment. Utilizing NAD^+ as an indispensable cofactor for *E. coli* DNA ligase to catalyze the ligation of two oligonucleotides, the electrochemical and molecular beacon (MB) based fluorescence biosensors have been reported for NAD^+ detection with detection limits down to 1.8 nM and 0.3 nM, respectively.[10] More recently, a novel ligation-triggered DNAzyme cascade method has also been developed for amplified fluorescence detection of NAD^+, resulting in a lower detection limit of 50 pM.[11] These assays exhibit high specificity in distinguishing NAD^+ from its analogs. However, such measurements are not sensitive enough for the detection of low-abundance NAD^+ in small amounts of biological samples. Therefore, the development of a novel and signal-amplified approach for further improving sensitivity is still an urgent demand.

Rolling circle amplification (RCA) is an isothermal DNA replication technique[12] and can amplify a short DNA primer to generate long linear single-stranded DNA (ssDNA) molecules containing many tandem repeated sequences which are complementary to the circular DNA template.[13] Due to its simplicity, robustness, high specificity, and powerful signal amplification,[14] RCA has received considerable attention as a highly versatile DNA amplification tool and has been widely applied in the ultrasensitive detection of DNA,[15] RNA,[14b,16] proteins,[17] as well as small molecules.[18] Herein, we developed a fluorescence sensing strategy for ultrasensitive and selective detection of NAD^+ by taking advantage of the great amplification capability of RCA and the extreme fidelity of *E. coli* DNA ligase toward its substrates. The designed strategy is depicted in Scheme 1. The ten 3′- and 5′-terminal bases of the 59-mer padlock probe were designed to be perfectly complementary to the half sequences of 20-mer DNA (cDNA) (see ESI†). In the presence of NAD^+, the *E. coli* DNA ligase could catalyze the ligation between 3′-OH and 5′-PO_4 ends of the padlock probes, triggering the formation of a circular DNA template. Using the cDNA as primer, RCA was subsequently initiated by the high-displacement activity of the phi29 DNA polymerase in the presence of dNTPs. The long ssDNA product containing tandem repeats was generated in large quantities by RCA and could serve as an excellent template for periodic binding of 29-mer MBs with partial loop regions complementary to the middle 15-mer units of each repeated sequence. This would result in the opening of the numerous MBs and produce the dramatic increase in fluorescent signals with very little quenching

[a] *Key Laboratory of Biomedical Information Engineering of Education Ministry, School of Life Science and Technology, Xi'an Jiaotong University, Xi'an, Shaanxi 710049, P. R. China. E-mail: yxzhao@mail.xjtu.edu.cn*
[b] *Shanghai Institute of Applied Physics, Chinese Academy of Sciences, Shanghai 201800, P. R. China. E-mail: fchh@sinap.ac.cn*

† Electronic supplementary information (ESI) available: Experimental details and supporting figures. See DOI: 10.1039/c2cc17422g

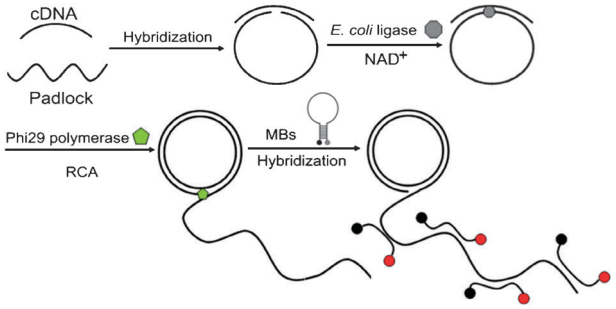

Scheme 1 Schematic representation of target-triggered ligation–rolling circle amplification (L-RCA) assay for nicotinamide adenine dinucleotide (NAD^+).

effect due to the effective spatial separation of the fluorophore and quencher not only within MBs but also between adjacent MBs on the ssDNA product. In contrast, in the absence of target NAD^+, *E. coli* DNA ligase would lose its catalysis activity for the ligation of padlock probes, and the RCA process could not proceed. Therefore, there was no fluorescence enhancement. In this way, we successfully converted each NAD^+-triggered ligation event into the detectable fluorescent signals, which were significantly amplified by RCA in an isothermal fashion.

Typical fluorescence spectra characteristics of the sensing strategy in response to NAD^+ are shown in Fig. S1 in ESI.† Compared with the background fluorescence of the MBs, 10 μM NAD^+ resulted in a significant fluorescence enhancement while a control experiment without NAD^+ only exhibited a negligible fluorescence change. The result provided a convincing proof of the detection mechanism of the proposed sensing strategy shown in Scheme 1.

In this novel strategy, RCA was a crucial step, which mediated the generation and amplification of the fluorescence signal. In order to achieve the system's best sensing performance, several experimental parameters affecting RCA were investigated (Fig. 1). The NAD^+ concentration was set at 5 μM for the subsequent optimizations. The NAD^+-triggered ligation reaction has a significant influence on the RCA process. The full hybridization equilibrium between the padlock probe and cDNA is a key factor for ensuring efficient ligation reaction. Therefore, the effect of molar ratio of the padlock probe to cDNA was evaluated using a fixed concentration of cDNA, namely 10 nM. As shown in Fig. 1a, the fluorescence intensity increased with the increase in molar ratio. When the ratio

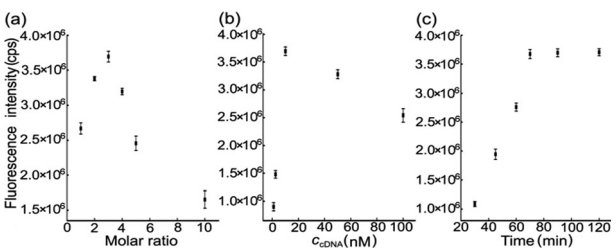

Fig. 1 Dependence of the fluorescence response of the sensing strategy on molar ratio of padlock probe to cDNA (a), the concentration of cDNA (b), and the reaction time of RCA (c). The concentration of target NAD^+ was 5 μM. Fluorescence intensity was recorded at 518 nm with an excitation wavelength of 495 nm. The error bar was calculated from three independent experiments.

value reached 3 : 1, the maximum fluorescence intensity was achieved. Thereafter, the fluorescence response exhibited a gradual decrease with a further increase in the molar ratio. This was probably because a large excess of padlock probes disturbed their hybridization with the cDNA in a head-to-tail fashion and the subsequent L-RCA reaction.[19] As a result, the molar ratio of 3 : 1 was selected for further investigation. The hybridization of cDNA with the padlock probe is a prerequisite for NAD^+-triggered ligation. In addition, cDNA also serves as a primer for RCA reaction after circularization of the padlock probe. Fig. 1b shows the variance of fluorescence intensity with the concentration of cDNA. Finally, 10 nM was selected as the optimal concentration due to its strongest fluorescence intensity. In theory, more complementary copies of the circular template are generated with the elongation of RCA reaction time; stronger signal amplification will be produced. So the effect of RCA reaction time on the fluorescence signal was examined, which is shown in Fig. 1c. The fluorescence intensity enhanced quickly with the increase in reaction time, and nearly reached a plateau after 70 min. This might be attributed to the fact that the RCA reaction had reached equilibrium caused by exhaustion of the RCA substrates or inactivation of phi29 DNA polymerase.[20] Therefore, 70 min was chosen as the optimum time for the RCA reaction. This time was in agreement with the reported RCA reaction time of 1–2 h.[20,21]

The feasibility of the fluorescent biosensor was verified by agarose gel electrophoresis and ethidium bromide staining. As shown in Fig. S2 in ESI†, the long ssDNA products of L-RCA triggered by NAD^+ were observed in lane 1 (10 nM NAD^+) and 2 (1 μM NAD^+), respectively, in which the RCA products showed extremely low mobility. A brighter band was observed in lane 2, indicating that the higher concentration of NAD^+ would result in generating more RCA products. In contrast, no band appeared in the absence of NAD^+ in lane 3, indicating no RCA products were generated in the control experiment. Although the experiments might not give a reliable assessment of the molecular weight of the RCA products due to difference in electrophoretic behavior between single-stranded and double-stranded DNA, they provided immediate evidence for the high molecular weight of the ssDNA products.[22] These results indicated that NAD^+ acted as a trigger of the RCA reaction and the signal enhancement had a positive correlation with the NAD^+ level.

Under the optimal conditions, the sensitivity of the sensing strategy was examined by fluorimetric titration. Fig. 2a depicts fluorescence emission spectra of the sensing system upon the addition of NAD^+ at different concentrations. The fluorescence intensities increased remarkably when the concentration of NAD^+ was raised from 0 pM to 5 μM, and then leveled off beyond 5 μM (data not shown). Fig. 2b shows the relationship between the fluorescence response and the different concentrations of target NAD^+. The change in fluorescence intensity (ΔF) was proportional to the logarithmic value of the NAD^+ concentration over a 6-decade range from 5 pM to 5 μM with a linear correlation coefficient of 0.9905. The detection limit, calculated as three times the signal-to-noise ratio, was 1 pM, which is remarkably lower than those of 0.3 nM for MB based bioassays, and 1.8 nM for an electrochemical biosensor,[10] and 50-fold lower than that for the ligation-triggered DNAzyme cascade method.[11] The ultrahigh sensitivity was attributed to the following factors. First, the

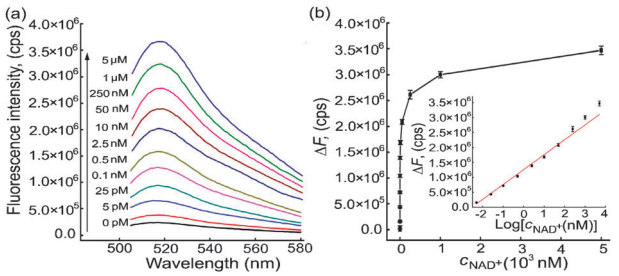

Fig. 2 (a) Fluorescence emission spectra recorded at different concentrations of target NAD^+. (b) Fluorescence intensity changes (ΔF) upon the addition of different concentrations of NAD^+. The inset of (b) displays the linear relationship between ΔF and the logarithmic value of the NAD^+ concentration (5 pM–5 μM). ΔF was calculated by $F - F_0$, where F and F_0 represent fluorescence intensity in the presence and absence of NAD^+, respectively. Error bars show the standard deviation of three experiments.

introduction of NAD^+ would trigger the ligation between 3′-OH and 5′-PO_4 ends of the padlock probe, and eventually the long ssDNA product containing many tandem repeated detection sites was generated in large quantities by RCA, substantially amplifying each target-triggered ligation event. Second, MBs showed relatively low background fluorescence and could be opened upon hybridization with the detection sites, which dramatically increased the fluorescence signal.

In addition to the detection sensitivity, specificity is another critical factor to evaluate the practicality of the fluorescent biosensor. The specificity of the sensing strategy was determined by challenging it with the NAD^+ analogs such as NADH, nicotinamide adenine dinucleotide phosphate ($NADP^+$), reduced nicotinamide adenine dinucleotide phosphate (NADPH), adenosine triphosphate (ATP), adenosine diphosphate (ADP) and adenosine 5′-monophosphate (AMP) respectively. Fig. 3 presents the histograms of fluorescence intensity for the blank and solutions containing NAD^+ (50 nM) and its analogs (10 μM). It could be observed that the NAD^+ analogs exhibited almost the same fluorescence response as the blank solution without NAD^+, and did not induce any significant signal. The results demonstrate that the proposed strategy exhibits high selectivity for NAD^+, which makes it promising for practical applications. The excellent specificity was attributed to the intrinsically extreme fidelity of *E. coli* DNA ligase for NAD^+.

In summary, a novel fluorescence sensing strategy for the ultrasensitive detection of NAD^+ was reported in this study. The method takes advantage of the intrinsically extreme fidelity of *E. coli* DNA ligase to NAD^+, the powerful signal amplification

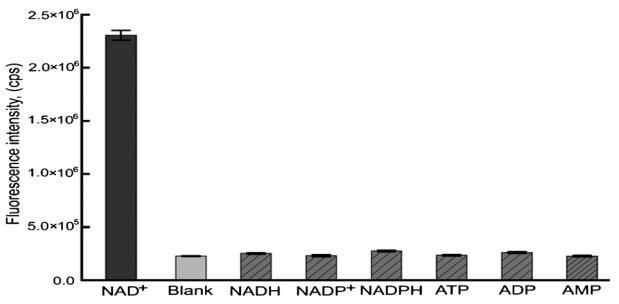

Fig. 3 The difference in fluorescence intensity between the blank and solutions containing NAD^+ and its analogs. Concentration of NAD^+: 50 nM, concentration of NAD^+ analogs: 10 μM.

capability of RCA and the significant increase in fluorescence signal associated with the specific hybridization of MBs with L-RCA products. By exploiting the strategy, each NAD^+-triggered ligation event is translated into a detectable fluorescence response. An extremely low detection limit as low as 1 pM for the target NAD^+ is achieved with a wide detection range of 6 orders of magnitude. The picomolar sensitivity is much lower than those of previously reported biosensors. At the same time, this proposed approach exhibits extreme specificity towards NAD^+, even against 200 times excess of NAD^+ analogs. In addition, it is worthwhile to point out that no sophisticated equipment is required. These advantages endow the NAD^+ sensing strategy with a great potential for practical applications without sample purification, despite the fact that our assay involves several separate steps which makes it a little complicated and time consuming (about 2.5 h).

This research was financially supported by the National Natural Science Foundation of China (21005059) and the Fundamental Research Funds for the Central Universities

Notes and references

1 (*a*) A. De Flora, S. Bruzzone, C. Usai, R. Graeff and H. C. Lee, *Biochem. J.*, 2003, **375**, 395; (*b*) M. C. Gendron, N. Schrantz, D. Metivier, G. Kromer, Z. Maciorowska, F. Sureau, S. Koester and P. X. Petit, *Biochem. J.*, 2001, **354**, 727; (*c*) S. L. McKnight, J. Rutter, M. Reick and L. C. Wu, *Science*, 2001, **293**, 510; (*d*) R. H. Goodman, Q. H. Zhang and D. W. Piston, *Science*, 2002, **295**, 1895; (*e*) W. Ying, *Front. Biosci.*, 2007, **12**, 1863; (*f*) L. Guarente, S. J. Lin and P. A. Defossez, *Science*, 2000, **289**, 2126.

2 (*a*) W. T. Penberthy and I. Tsunoda, *Curr. Pharm. Res.*, 2009, **15**, 64; (*b*) A. Wilkinson, J. Day and R. Bowater, *Mol. Microbiol.*, 2001, **40**, 1241.

3 M. J. Charron and S. Bonner-Weir, *Nat. Med.*, 1999, **5**, 269.

4 C. Bernofsk and M. Swan, *Anal. Biochem.*, 1973, **53**, 452.

5 E. S. Yeung, W. J. Xie and A. S. Xu, *Anal. Chem.*, 2009, **81**, 1280.

6 K. Yamada, N. Hara, T. Shibata, H. Osago and M. Tsuchiya, *Anal. Biochem.*, 2006, **352**, 282.

7 F. Sadanaga-Akiyoshi, H. Yao, S. Tanuma, T. Nakahara, J. S. Hong, S. Ibayashi, H. Uchimura and M. Fujishima, *Neurochem. Res.*, 2003, **28**, 1227.

8 D. A. Sinclair, R. M. Anderson, M. Latorre-Esteves, A. R. Neves, S. Lavu, O. Medvedik, C. Taylor, K. T. Howitz and H. Santos, *Science*, 2003, **302**, 2124.

9 P. J. Hergenrother and K. S. Putt, *Anal. Biochem.*, 2004, **326**, 78.

10 (*a*) K. M. Wang, X. X. He, X. Q. Ni, Y. H. Wang and L. X. Jian, *Talanta*, 2011, **83**, 937; (*b*) K. M. Wang, Z. W. Tang, P. Liu, C. B. Ma, X. H. Yang, W. H. Tan and X. Y. Lv, *Anal. Chem.*, 2011, **83**, 2505.

11 L. M. Lu, X. B. Zhang, R. M. Kong, B. Yang and W. H. Tan, *J. Am. Chem. Soc.*, 2011, **133**, 11686.

12 A. Fire and S. Q. Xu, *Proc. Natl. Acad. Sci. U. S. A.*, 1995, **92**, 4641.

13 Y. F. Li, M. M. Ali, S. D. Aguirre, Y. Q. Xu, C. D. M. Filipe and R. Pelton, *Chem. Commun.*, 2009, 6640.

14 (*a*) U. Landegren, J. Baner, M. Nilsson and M. Mendel-Hartvig, *Nucleic Acids Res.*, 1998, **26**, 5073; (*b*) Z. P. Li, Y. Q. Cheng, X. Zhang, X. X. Jiao, Y. C. Wang and Y. L. Zhang, *Angew. Chem., Int. Ed.*, 2009, **48**, 3268.

15 T. Kitamori, K. Sato, A. Tachihara, B. Renberg, K. Mawatari, K. Sato, Y. Tanaka, J. Jarvius and M. Nilsson, *Lab Chip*, 2010, **10**, 1262.

16 Y. T. Zhou, Q. Huang, J. M. Gao, J. X. Lu, X. Z. Shen and C. H. Fan, *Nucleic Acids Res.*, 2010, **38**, e156.

17 C. A. Savran, J. Lee, K. Icoz, A. Roberts and A. D. Ellington, *Anal. Chem.*, 2010, **82**, 197.

18 Y. F. Li and M. M. Ali, *Angew. Chem., Int. Ed.*, 2009, **48**, 3512.

19 Z. S. Wu, S. B. Zhang, H. Zhou, G. L. Shen and R. Q. Yu, *Anal. Chem.*, 2010, **82**, 2221.

20 W. Cheng, F. Yan, L. Ding, H. X. Ju and Y. B. Yin, *Anal. Chem.*, 2010, **82**, 3337.

21 J. Hu and C. Y. Zhang, *Anal. Chem.*, 2010, **82**, 8991.

22 L. Zhou, L. J. Ou, X. Chu, G. L. Shen and R. Q. Yu, *Anal. Chem.*, 2007, **79**, 7492.

